ELSEVIER

Journal of Power Sources 74 (1998) 46–53

JOURNAL OF POWER SOURCES

Preparation of $Li_yMn_xNi_{1-x}O_2$ as a cathode for lithium-ion batteries

Masaki Yoshio [a,*], Yanko Todorov [a], Kohji Yamato [a], Hideyuki Noguchi [a], Jun-ichi Itoh [a], Masaki Okada [b], Takashi Mouri [b]

[a] *Department of Applied Chemistry, Saga University, Saga 840, Japan*
[b] *Nanyoh Research Center, Tohso, Shinnanyoh 746, Japan*

Received 5 August 1997; accepted 6 December 1997

Abstract

The preparation of $Li_yMn_xNi_{1-x}O_2$ from $LiOH \cdot H_2O$, $Ni(OH)_2$ and γ-MnOOH under oxygen and flowing air is studied. Single phases of $Li_yMn_xNi_{1-x}O_2$ ($0 < x < 0.3$ in O_2, $0 < x < 0.2$ in air) are prepared by using γ-MnOOH as a manganese source. The optimum heating temperatures are 800°C for $x = 0.1$ and 850°C for $x = 0.2$. The particle size of the source manganese compound is an important factor for the preparation of the single phase $Li_yMn_xNi_{1-x}O_2$. It is found that $Li_yMn_xNi_{1-x}O_2$ is formed from Li_yNiO_2 and Li_2MnO_3 at a temperature higher than 750°C. As the average valence of transition metals (Mn and Ni) for $Li_yMn_xNi_{1-x}O_2$ obtained under flowing oxygen is found to be more than 3, it is experimentally confirmed that manganese in $Li_yMn_xNi_{1-x}O_2$ exists as both Mn(III) and Mn(IV). For this reason, the presence of $Li_yMn_xNi_{1-x}O_2$ would be allowed for a wide range of y, for example, $0.99 < y < 1.10$ for $Li_yMn_{0.1}Ni_{0.9}O_2$.

Keywords: Cathode material for lithium-ion batteries; $Li_yMn_xNi_{1-x}O_2$; Optimum preparation condition; Formation process; Electrochemical property

1. Introduction

The layered $LiNiO_2$ has been used as a cathode material with a relatively low cost and high capacity for lithium-ion batteries [1–8], however, there are two important problems for such a cathode. One problem is the difficulty in preparation of the electroactive $LiNiO_2$ because its discharge capacity depends strongly on the Li/Ni ratio in Li_xNiO_2, cation disorder, and the oxidation state of nickel. The other problem is the poor cycle life of the $LiNiO_2$ electrode when it is charged to a higher voltage (4.3 V vs. Li^+/Li) for withdrawing a higher capacity. The NiO_2 phase is formed at the end of the charging process in the $LiNiO_2$ electrode. An appreciable volume change during the transformation from rhombohedral $Li_{0.75}NiO_2$ to the rhombohedral NiO_2 phase [6–8] would cause the poor cycle life of the electrode. To avoid the formation of the NiO_2 phase, the discharge capacity must be kept constant. For this purpose, substitution of Ni by Al [9] or Fe [10] has been tried. In this study, we have attempted to overcome these disadvantages of $LiNiO_2$ by substituting part of the Ni by Mn.

Substitution of Ni by Mn(II) using MnO or $MnCO_3$ has been investigated by Rossen et al. [11] and Nitta et al. [12]. They have noticed that this compound shows poor cycleability, and have suggested that the valence of Mn in $LiMn_xNi_{1-x}O_2$ is 2, which is same as the valence of the starting material $MnCO_3$.

In this study, we selected a trivalent manganese compound, γ-MnOOH, as the manganese source. The resulting $LiMn_xNi_{1-x}O_2$ compounds display excellent battery performance. The compounds were synthesized in an O_2 atmosphere. Further, it is found that the Li/(Mn + Ni) ratio does not affect the discharge capacity of $Li_yMn_{0.1}Ni_{0.9}O_2$ over the wide range of $0.99 < y < 1.1$. In terms of industrial production, it is also important that the electroactive $LiMn_{0.2}Ni_{0.8}O_2$ is produced in an air atmosphere.

2. Experimental

Two manganese compounds, γ-MnOOH and MnO_2 [IC (International Common MnO_2 Sample) No. 17-Mitsui Mining and Smelting] were used as the manganese sources. γ-MnOOH was supplied by Tohso and is composed of very fine, needle-like particles of diameter 1–3 μm [13].

* Corresponding author.

0378-7753/98/$19.00

$LiOH \cdot H_2O$ (2.174 g), $Ni(OH)_2$ (4.231 g) and γ-MnOOH (0.466 g) or MnO_2 (0.461 g) were mixed ($x = 0.1$) and ground using a mortar. The mixture was pressed into discs at 800 kg cm^{-2}. The discs were heated under flowing oxygen (~ 60 ml/min) or in air at 700–850°C for 24 h.

Crystallographic characterization of the samples and their delithiated products was carried out using a Rigaku diffractometer (RINT 1000) with FeKα radiation. Izumi's Rietveld program (RIETAN) [14] was used for the analysis of the powder diffraction profiles.

The total content of Ni and Mn was determined by complexometry. A 0.5 g sample of $Li_yMn_xNi_{1-x}O_2$ was dissolved in concentrated HCl solution and the resulting solution was diluted with distilled water to 100 ml. A 5-ml portion of this solution was mixed with 0.4 mmol of EDTA (ethylenediamine-tetraacetic acid) at pH = 10 and diluted to 100 ml. An excess of EDTA was titrated with 0.01 mol/dm^3 zinc acetate solution using Xyrenol orange as an indicator. The content of nickel was determined by gravimetry with dimethylglyoxime. The content of Mn was calculated from the above data. The lithium content was determined by atomic absorption spectroscopy.

The oxidizing power of the sample [15] was determined by iodometry after dissolving it (200 mg) in 100 ml of 2 M HCl solution containing 3 g KI under an argon atmosphere.

The charge and discharge characteristics of $Li_yMn_xNi_{1-x}O_2$ cathodes were examined in a laboratory cell. The cell is comprised of cathode and lithium metal anode, separated by a polypropylene separator and a glass-fibre mat. The cathode consisted of 20 mg of $Li_yMn_xNi_{1-x}O_2$ and 12 mg conducting binder [13], pressed on a stainless-steel screen at 800 kg cm^{-2} and dried at 200°C for 24 h. The electrolyte solution was 1 M $LiPF_6$/PC (propylene carbonate) and DEC (diethylcarbonate). The PC and DEC were mixed in a 1:4 volume ratio. The cell was cycled in the voltage range of 3.0–4.3 V at a current density of 0.4 mA cm^{-2}.

The OCV (open circuit voltage) values were taken after equilibration for 4 days.

3. Results and discussion

3.1. Preparation of single phase $LiMn_xNi_{1-x}O_2$ under flowing oxygen

The XRD patterns of the products ($x = 0.1$ and $x = 0.2$) obtained using MnO_2 or γ-MnOOH as the manganese source are shown in Fig. 1. Single-phase $LiMn_xNi_{1-x}O_2$ ($x = 0.1$ and $x = 0.2$) with space group $R\bar{3}$ can be obtained only from γ-MnOOH. The product prepared from MnO_2 (IC 17) contains Li_2MnO_3 in the temperature range 750 to 850°C, as described by Rossen et al. [11]. These results indicate that the manganese source is very important for preparing a single-phase $LiMn_xNi_{1-x}O_2$ compound. Nevertheless, the valence of the manganese source is not important because both Mn(II) [11] and Mn(III) compounds form a single-phase $LiMn_xNi_{1-x}O_2$. In fact, this compound is formed by the reaction between Li_xNiO_2 and Li_2MnO_3, as will be described later. In the case of MnO_2, this reaction does not proceed smoothly. Nitta et al. [12] used $MnCO_3$ as the manganese source, but it decomposes easily to MnO_2 below 400°C. Therefore, $LiMn_xNi_{1-x}O_2$ would be formed via Li_2MnO_3 even if $MnCO_3$ is used as the manganese source.

Lithium–manganese oxides formed from γ-MnOOH and $LiNO_3$ or MnO_2 and $LiNO_3$ by the melt-impregnation method have the same particle size as the manganese sources [13,16], therefore, except for valency, the main difference between γ-MnOOH and MnO_2 (IC 17) is in particle size. The mean particle size of IC 17 is ~ 40 μm, which is much larger than that of γ-MnOOH (0.2–0.4 μm in diameter, a 1–2 μm in length) [13]. Our results show

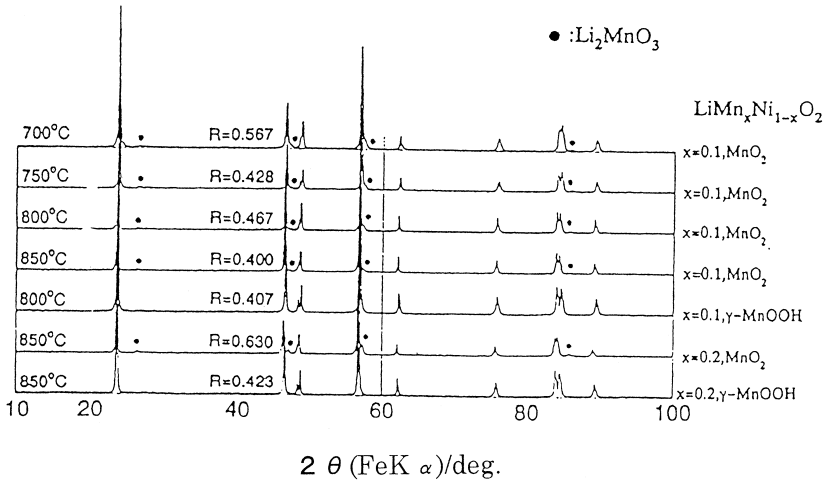

Fig. 1. XRD patterns of products ($x = 0.1$ and $x = 0.2$) obtained by using MnO_2 or γ-MnOOH as a manganese source.

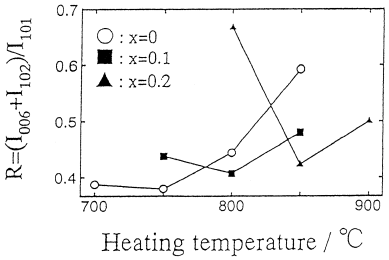

Fig. 2. Relation between R value of $LiMn_xNi_{1-x}O_2$ ($x = 0$, 0.1 and 0.2) and heating temperature.

that the particle size of the source manganese compounds is an important factor in obtaining a single-phase $LiMn_xNi_{1-x}O_2$.

Fig. 2 shows the (012,006)/(101) intensity ratios (R value proposed by Reimers et al. [10]) of $LiMn_xNi_{1-x}O_2$ vs. heating temperature. $LiNiO_2$ shows the lowest R value of 3.67 at 750°C and many researchers have prepared excellent electroactive $LiNiO_2$ by heat treatment at 750°C in an oxygen atmosphere. The optimum heating temperature for the preparation of the layered $LiMn_xNi_{1-x}O_2$ is determined from the R value. When x is increased, an elevated heating temperature is desirable to prepare a single-phase compound with a lower cation disorder. The optimum heating temperature is 800°C for $x = 0.1$, and 850°C for $x = 0.2$. These results show that heating temperature significantly affects the degree of cation disorder in $LiMn_xNi_{1-x}O_2$ and should be optimized for preparing a layered compound with a lower cation disorder. Kanno et al. [7] indicated that $LiNiO_2$ decomposes to $Li_{1-x}Ni_{1+x}O_2$ at a higher temperature (> 750°C). The increase in the R value of $LiNiO_2$, prepared above 800°C is explained by the above observation. The increase in the R value of $LiMn_xNi_{1-x}O_2$ also indicates the decomposition of the compound at high temperatures.

Table 1
Hexagonal lattice parameter and percentage of Ni and Mn in Li layer (determined by Rietveld Analysis) of $LiMn_xNi_{1-x}O_2$ prepared in O_2

Compound	a (Å)	c (Å)	Ni + Mn in Li layer (%)
$LiNiO_2$	2.879	14.209	1.2
$LiMn_{0.1}Ni_{0.9}O_2$	2.874	14.213	1.3
$LiMn_{0.2}Ni_{0.8}O_2$	2.879	14.234	4.8

Lattice parameters and the degree of cation disorder in $LiMn_xNi_{1-x}O_2$ were determined by Rietveld analysis. The results of the Rietveld refinement for $LiMn_{0.2}Ni_{0.8}O_2$ based on the $LiNiO_2$ structure are given in Fig. 3. The differences between the calculated and observed intensity are shown in the lower part of the figure. Small differences between both intensities and R_{WP} [14] of 16–18% would show a successful refinement. The lattice parameter and degree of cation disorder (expressed by a transition metal (Ni + Mn) in the Li layer) for $LiMn_xNi_{1-x}O_2$ ($x = 0$, 0.1 and 0.2) prepared at the optimum temperature are summarized in Table 1.

The hexagonal lattice parameters a and c of $LiMn_xNi_{1-x}O_2$ ($x = 0.1$ and $x = 0.2$) are 2.874–2.879 Å and 14.213–14.234 Å, respectively. The refined lattice parameters a are nearly the same as those ($a = 2.874$ Å and $c = 14.184$–14.194 Å) for $Li_{1.1}Mn_xNi_{1-x}O_2$ ($x = 0.1$ and 0.2) [11], but parameters c are slightly longer than those reported.

The degree of cation disorder in $LiMn_{0.1}Ni_{0.9}O_2$ is 1.3% and the same as that in $LiNiO_2$ (1.2%). By contrast, the disorder in $LiMn_{0.2}Ni_{0.8}O_2$ is four times higher than that in $LiNiO_2$ or $LiMn_{0.1}Ni_{0.9}O_2$. Clearly, substitution of Ni by Mn causes an increase in the degree of cation disorder in $LiMn_xNi_{1-x}O_2$. Rossen et al. [11] have re-

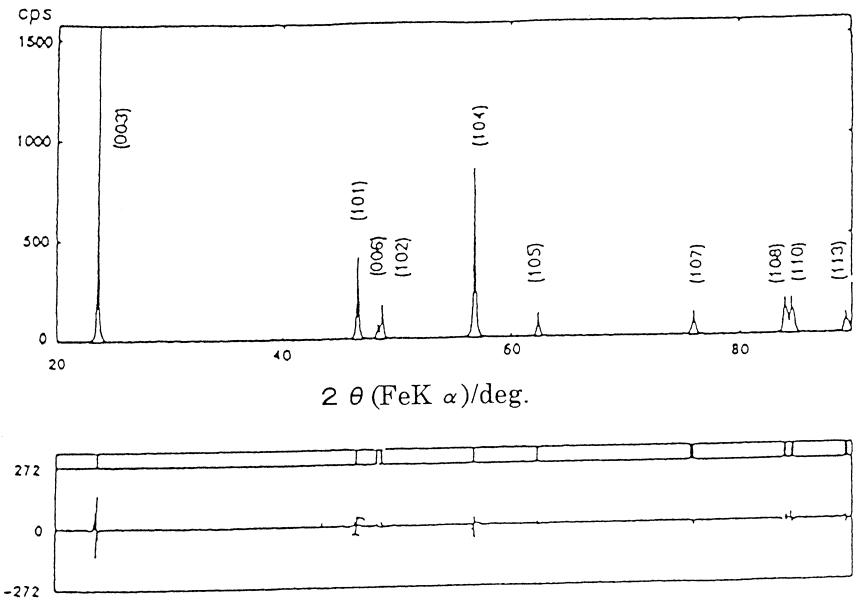

Fig. 3. Rietveld analysis of $LiMn_{0.2}Ni_{0.8}O_2$.

Table 2
Hexagonal lattice parameter and percentage of Ni and Mn in Li layer (determined by Rietveld Analysis) of $LiMn_xNi_{1-x}O_2$ prepared in air

Compound	a (Å)	c (Å)	Ni + Mn in Li layer (%)
$LiNiO_2$	2.883	14.204	6.2
$LiMn_{0.1}Ni_{0.9}O_2$	2.884	14.224	8.7
$LiMn_{0.2}Ni_{0.8}O_2$	2.883	14.248	7.2

ported that the degree of cation disorder in $Li_{1.1}Mn_xNi_{1-x}O_2$. $(0.1 > x > 0.5)$ is more than 5% and increases with increase in x. This slightly higher value is due to an inadequate heating temperature for the preparation of $LiMn_xNi_{1-x}O_2$.

3.2. Preparation of single-phase $LiMn_xNi_{1-x}O_2$ in air

We have found that single-phase $LiMn_xNi_{1-x}O_2$ (x = 0.1 and 0.2) can be prepared in air containing CO_2 and moisture. This finding is very important from an industrial point of view because a special production system would not be required. The degrees of cation disorder in $LiMn_xNi_{1-x}O_2$ ($x = 0$, 0.1 and 0.2) are summarized in Table 2. The values for the compounds prepared in air exceed 6% and are much higher than those for compounds prepared in oxygen. Thus, difference in cation disorder becomes smaller when $x = 0.2$.

The average valence of Ni and Mn in $LiMn_xNi_{1-x}O_2$ prepared in O_2 and in air is presented in Fig. 4. The average valences of the compounds prepared in O_2 (2.98–3.05) are higher than those prepared in air (2.89–2.92) over the range $x = 0$ to $x = 0.3$. The highest values are observed at $x = 0.2$ for $LiMn_xNi_{1-x}O_2$ prepared in O_2 and at $x = 0.1$–0.2 for the material prepared in air. The oxidation of $LiMn_xNi_{1-x}O_2$ is accelerated both by an increase in the partial pressure of oxygen and by substitution of Ni by Mn. Arai et al. [4] reported that $LiNiO_2$ should be expressed as $Li_{1-x}Ni_{1+x}O_2$. This formula means that a Ni(II) rich sample has considerable cation disorder and, thus, the oxidation of Ni(II) to Ni(III) is essential to get layered $LiNiO_2$ without cation disorder.

3.3. Formation process of $LiMn_xNi_{1-x}O_2$

Fig. 5 shows the formation process of $LiMn_xNi_{1-x}O_2$ from $Ni(OH)_2$, $LiOH \cdot H_2O$ and γ-MnOOH. $Ni(OH)_2$ decomposes to NiO with the evolution of H_2O at 240°C. γ-MnOOH transforms to β-MnO_2 in air at 260°C. β-MnO_2 forms Li_2MnO_3 in the presence of an excess amount of LiOH at ~400°C, therefore, the main products of a $Ni(OH)_2$, LiOH and γ-MnOOH (Ni:Mn:Li = 0.8:0.2:1 in atomic ratio) mixture at 430°C are composed of NiO and Li_2MnO_3, as shown in Fig. 6. Li_2CO_3 is formed by the reaction of LiOH with CO_2 in air.

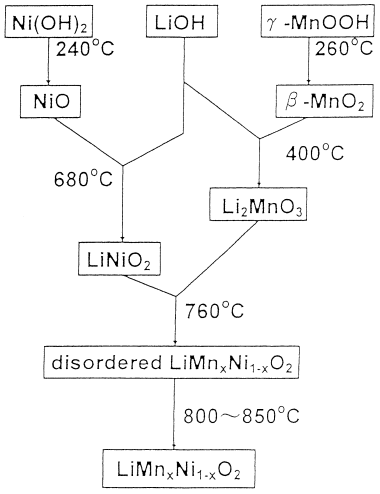

Fig. 5. Formation process of $LiMn_xNi_{1-x}O_2$.

Fig. 7 presents the TG-DSC analysis of: (a) a preheated sample and (b) a mixture of $LiOH \cdot H_2O$ and NiO. Three endothermic peaks (Fig. 7(b)) are observed for this mixture, at ~80°C, 420–440°C and 700°C (Li:Ni = 1:1 in atomic ratio). $LiOH \cdot H_2O$ loses crystalline water at ~70°C with a weight loss and melts at 420–440°C. The peak at 695°C is due to the formation of $LiNiO_2$ from LiOH and NiO. Weight loss at a temperature above 800°C indicates decomposition of $LiNiO_2$ with loss of lithium. [5] The preheated sample gives two endothermic peaks at 680 and 760°C. The peak at 680°C agrees well with the temperature of the peak assigned to the formation of $LiNiO_2$. The new peak at 760°C can be assigned to the formation of $LiMn_xNi_{1-x}O_2$ from $LiNiO_2$ and Li_2MnO_3. Since this process proceeds in the solid state, the particle size of Li_2MnO_3 is a very important factor in obtaining a single-phase $LiMn_xNi_{1-x}O_2$. The presence of Li_2MnO_3

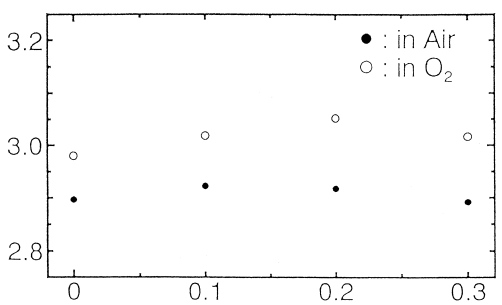

Fig. 4. Average valence of transition metal (Mn and Ni) for $LiMn_xNi_{1-x}O_2$ ($x = 0$–0.3) prepared in air and O_2.

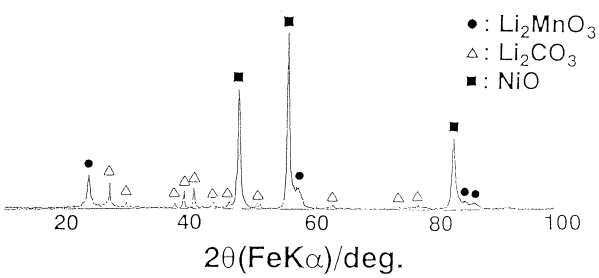

Fig. 6. XRD pattern of $LiOH \cdot H_2O$, NiO and γ-MnOOH mixture heated at 430°C for 24 h.

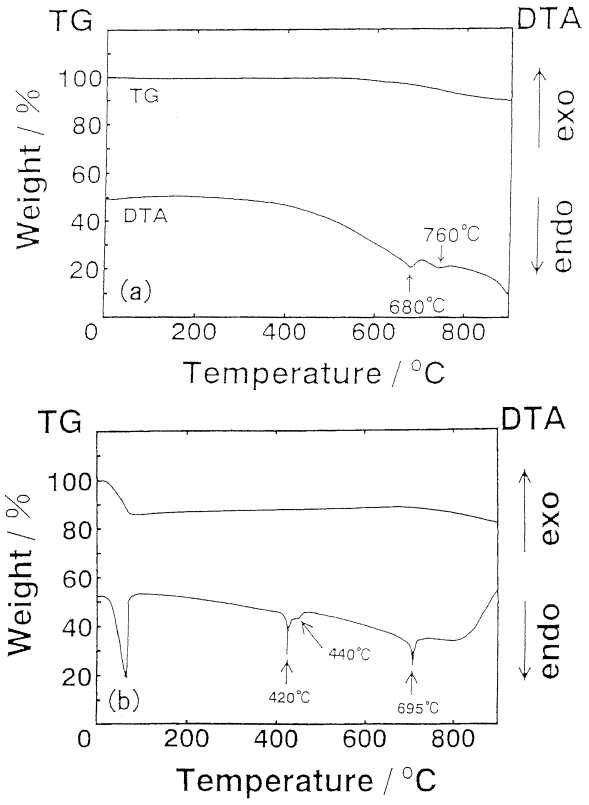

Fig. 7. TG-DTA curves for (a) a preheated mixture of $LiOH \cdot H_2O$, NiO and γ-MnOOH at 430°C and (b) $LiOH \cdot H_2O$ and NiO.

as an impurity in $LiMn_xNi_{1-x}O_2$ is easily understood from this reaction scheme.

3.4. Electrochemical properties of $LiMn_xNi_{1-x}O_2$ prepared in O_2

Fig. 8 shows the initial charge–discharge curves of $LiMn_xNi_{1-x}O_2$ ($x = 0$, $x = 0.1$ and $x = 0.2$) prepared in flowing oxygen at the optimum heating temperature. The charge–discharge curves of $LiNiO_2$ resemble those reported earlier. Substitution of Ni by Mn causes an increase in the charge voltage at $y > 0.4$ in $Li_yMn_xNi_{1-x}O_2$ and a decrease in the initial charge capacities of $LiMn_xNi_{1-x}O_2$. A complex discharge curve is replaced by a simple discharge curve. This is made clear by observation of the chronopotentiograms shown in Fig. 9, the compounds are different from each other: $LiMn_{0.2}Ni_{0.8}O_2$ shows only one peak at ~3.77 V during charge while multiple peaks (at 3.68, 3.82, 4.01 and 4.20 V) are observed for $LiNiO_2$. These peaks correspond to various phase transformations [6–8]. The presence of a monoclinic phase and rhombohedral NiO_2 phase are determined by XRD analysis. The chronopotentiogram of $LiMn_{0.1}Ni_{0.9}O_2$ has an intermediate character between $LiNiO_2$ and $LiMn_{0.2}Ni_{0.8}O_2$. It is composed of three peaks at 3.73, 4.05 and 4.22 V. The substitution of Ni by Mn causes an increase in peak voltage, and a decrease in the peak height and sharpness. Its effect is remarkable for the peaks at 3.82 and 4.05 V in $LiNiO_2$. Both $LiNiO_2$ and $LiMn_{0.1}Ni_{0.9}O_2$ have low cation disorder and, thus, layering with a low cation disorder forms a monoclinic phase and rhombohedral phase during charge–discharge cycles.

The cycleabilities of $LiMn_xNi_{1-x}O_2$ ($x = 0$, $x = 0.1$ and $x = 0.2$) are shown in Fig. 10. The discharge capacities for $x = 0.1$ or $x = 0.2$ are maintained at more than 150 mAh g^{-1} over 40 cycles. The $LiNiO_2$ delivers a higher discharge capacity of ~190 mAh g^{-1} in initial cycles, but its capacity goes down to 160 mAh g^{-1} at the 50th cycle. The rate of decline in capacity is higher than that for $LiMn_{0.1}Ni_{0.9}O_2$ or $LiMn_{0.2}Ni_{0.8}O_2$. It is concluded that substitution of Ni by Mn is effective for improving the cycleability of the $LiNiO_2$ electrode.

Evaporation of lithium is an important problem when preparing $LiNiO_2$. Since Li_xNiO_2 displays excellent bat-

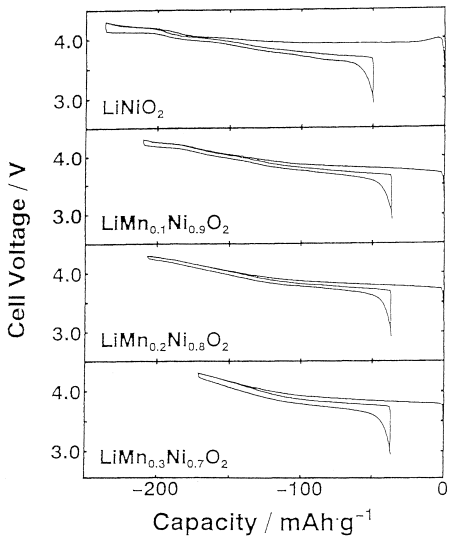

Fig. 8. Initial charge–discharge curves of $LiMn_xNi_{1-x}O_2$ ($x = 0$–0.03) prepared in O_2.

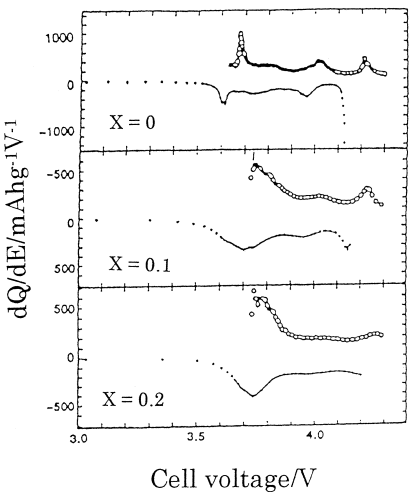

Fig. 9. Chronopotentiograms of $LiMn_xNi_{1-x}O_2$ ($x = 0$–0.2) prepared in O_2.

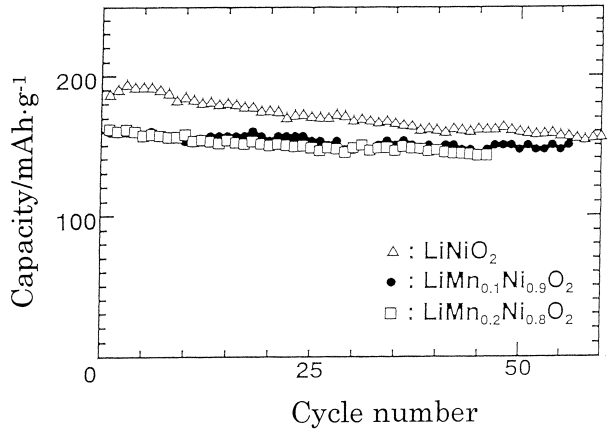

Fig. 10. Cycling performance of $LiMn_xNi_{1-x}O_2$ ($x = 0$–0.2) electrode.

tery performance at $x = 0.98$ [17], the effect of lithium content y in $Li_yMn_xNi_{1-x}O_2$ on battery performance was examined at around the stoichiometric amount of Li. The initial discharge capacities of $Li_yMn_xNi_{1-x}O_2$ are shown in Fig. 11. $Li_yMn_{0.1}Ni_{0.9}O_2$ delivers a fairly constant capacity of 160 mAh g^{-1} for the wide range of y from 0.99 to 1.10. This result is very important because it means that the problem of lithium evaporation is resolved. In other words, we can reproducibly prepare excellent $Li_yMn_{0.1}Ni_{0.9}O_2$ without controlling the lithium amount and heating condition very precisely.

The lower limit of y might correspond to the stoichiometric Li content and the higher limit might correspond to the Mn content. If manganese can exist as both Mn(III) and Mn(IV) in $Li_yMn_xNi_{1-x}O_2$ as proposed by Reimers et al. [10], the valence of manganese in $Li_{1.1}Mn_{0.1}Ni_{0.9}O_2$ is calculated as 4 under the assumption that Ni is 3.

In order to determine the chemical formula, samples with a nominal composition of $Li_{1.05}Mn_{0.1}Ni_{0.9}O_2$ and $Li_{1.05}Mn_{0.2}Ni_{0.8}O_2$ were chemically analyzed. Their chemical compositions are summarized in Table 3. The valence of manganese is calculated under the assumption that the valence of Ni equals 3. The data show that ~ 0.20% of Mn exists as Mn(III). It was contained experimentally that manganese exists as both Mn(III) and Mn(IV).

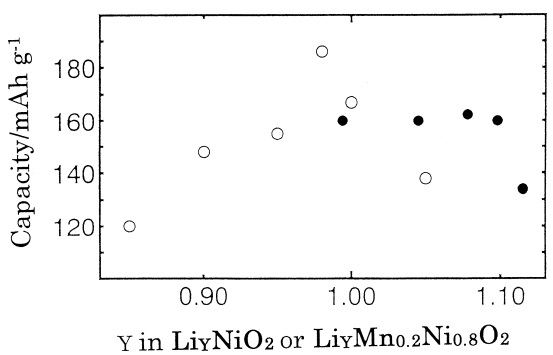

Fig. 11. Effect of Li content, y, in (●) $Li_yMn_xNi_{1-x}O_2$ and (○) Li_yNiO_2 on the initial discharge capacity.

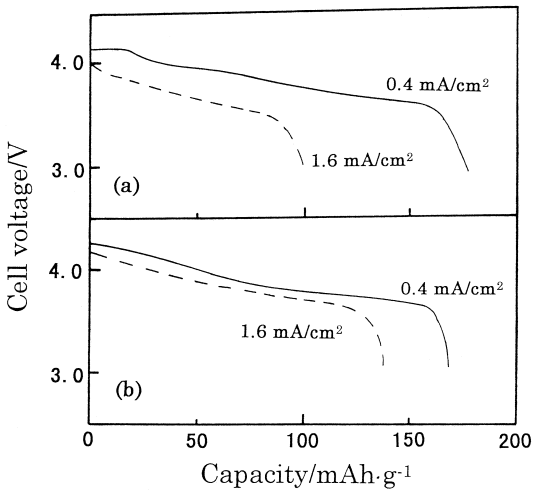

Fig. 12. Discharge capacity of (a) $LiNiO_2$ and (b) $LiMn_{0.2}Ni_{0.8}O_2$.

The effect of the charge–discharge rate on battery performance is examined for $LiMn_{0.2}Ni_{0.8}O_2$, which shows the smallest deviation between charge and discharge curves, and $LiNiO_2$ as shown in Fig. 12. Its discharge capacity at 0.4 and 1.6 mA cm^{-2} is 160 and 140 mAh g^{-1}, respectively. On the other hand, those of $LiNiO_2$ are 190 and 100 mAh g^{-1}, respectively. This means that the substitution of Ni by Mn is effective for improving the high-rate capability.

3.5. Battery performance of $LiMn_xNi_{1-x}O_2$ prepared in air

Fig. 13 shows the initial charge–discharge curves of $LiMn_xNi_{1-x}O_2$ ($x = 0$, 0.1 and 0.2) prepared in air.

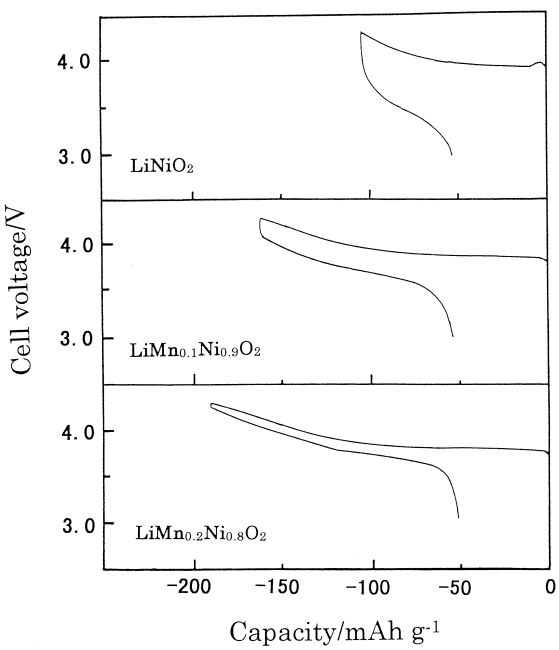

Fig. 13. Initial charge–discharge curves of $LiMn_xNi_{1-x}O_2$ ($x = 0$–0.2) electrodes.

Table 3
Calculated chemical formula, average valence of Ni and Mn, and ratio[a] of Mn(III) and Mn(IV) for $Li_yMn_xNi_{1-x}O_2$, based on chemical analysis

Calculated chemical formula	Average valence of Ni and Mn	Ratio of Mn(III) and Mn(IV)
$Li_{1.045}Mn_{0.104}Ni_{0.896}O_{2.031}$	3.019	Mn(III):0.82, Mn(IV):0.18
$Li_{1.026}Mn_{0.230}Ni_{0.770}O_{2.039}$	3.052	Mn(III):0.77, Mn(IV):0.23

[a]Valence of Ni is assumed as +3.

Though these samples have nearly the same cation disorder, viz., (6–8%), Table 3, their discharge capacities differ dramatically. The $LiMn_{0.2}Ni_{0.8}O_2$ delivers a capacity of more than 140 mAh g^{-1}, but the $LiNiO_2$ delivers a capacity of only 40 mAh g^{-1} with high polarization. The substitution of Ni by Mn decreases the polarization, so $LiMn_xNi_{1-x}O_2$ with a high cation disorder would show an excellent battery performance.

3.6. Electrochemical reaction of $LiMn_{0.2}Ni_{0.8}O_2$

The potential of the charge–discharge curves of $LiMn_{0.2}Ni_{0.8}O_2$ changes monotonously, which is different from the electrochemical behaviour of $LiNiO_2$. In order to determine its electrochemical reaction, the OCV and XRD of $Li_{1-z}Mn_{0.2}Ni_{0.8}O_2$ formed by the electrochemical oxidation of $LiMn_{0.2}Ni_{0.8}O_2$ have been measured.

Fig. 14 shows the OCV curves of $LiMn_{0.2}Ni_{0.8}O_2$ prepared in (a) oxygen and (b) in air during initial charge. Since both samples give similar OCV curves, slight differences in the degree of cation disorder and oxidation state of the transition metal would not influence the electrochemical reaction during the charge–discharge process. As the potential of $Li_{1-z}Mn_{0.2}Ni_{0.8}O_2$ changes continuously in the range from $z = 0$ to 0.55, only one reaction occurs in this region. When z exceeds 0.55, the OCV increases markedly and reaches a constant value of 4.15 V. XRD was performed in order to obtain further information about the electrochemical reaction. Fig. 15 shows the XRD pattern of $LiMn_{0.2}Ni_{0.8}O_2$ prepared in air. As there is no splitting in the (101) and (104) peaks, a monoclinic phase [6–8] does not appear during the charge–discharge cycles. All peaks shift continuously, so a homogeneous topotactic reaction occurs in the range from $z = 0$ to 0.8. The shift of the (006) peak at $2\Theta \approx 48°$ is unusual: the shift is to a lower angle until $z = 0.55$ and to a higher angle beyond 0.55. This means that the *c*-axis shrinks after the expansion. The lattice parameters *a* and *c* and lattice volume are calculated to understand in detail the change during de-intercalation. The lattice volume decreases continuously after the rapid increase at around $z = 0$, as shown in Fig. 16. The shrinkage of the *a*-axis is attributed predominantly to the volume change for $0.05 < z < 0.55$, however that of *c* decreases the lattice volume beyond $z = 0.6$. The *c*-axis shows a maximum value of 14.48 Å at $z = 0.55$. Such phenomena are reported for $LiNiO_2$ by Dahn [6]. The maximum monoclinic *a*-axis ($z = 0.5$) recalculated as hexagonal *c* is 14.51 Å (14.51 sin (90.5)), which is nearly the same as the maximum *c* of $LiMn_{0.2}Ni_{0.8}O_2$. As mentioned before, the lattice volume of $Li_{1-z}Mn_{0.2}Ni_{0.8}O_2$ can decrease continuously in the range from $z = 0.55$ to $z = 0.2$. On the other hand, $Li_{1-z}NiO_2$ maintains a con-

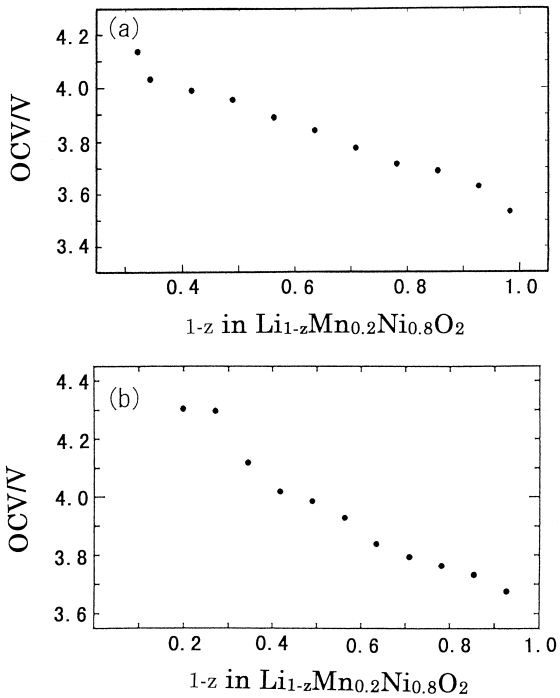

Fig. 14. OCV curves of $LiMn_{0.2}Ni_{0.8}O_2$ prepared in (a) O_2 and (b) air during initial charge.

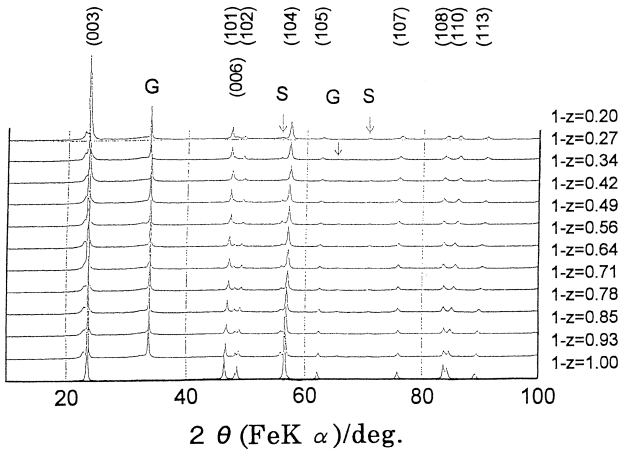

Fig. 15. XRD patterns of delithiated product, $Li_{1-z}Mn_{0.2}Ni_{0.8}O_2$, for $LiMn_{0.2}Ni_{0.8}O_2$ prepared in air during initial charge.

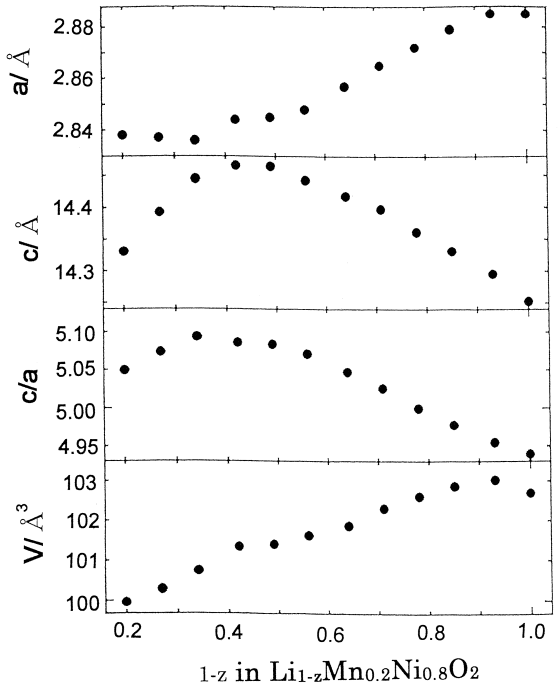

Fig. 16. Change in lattice parameters, a and c, c/a and lattice volume, V, for $LiMn_{0.2}Ni_{0.8}O_2$ prepared in air during initial charge.

stant volume of 102 Å [3]. Such a continuous decrease in lattice volume might protect against the formation of NiO_2 phase and it might be caused by oxidation of the transition metal in the lithium layer. Though the presence of a transition metal in the lithium layer for $LiNiO_2$ causes poor battery performance [3], its effect in $LiMn_xNi_{1-x}O_2$ does not become predominant because substitution of Ni by Mn decreases the polarization.

4. Conclusions

Substitution of Ni by Mn in $LiNiO_2$ exerts a strong affect on the electrochemical properties, i.e.,

(i) the lithium content $0.99 < y < 1.10$ in $Li_yMn_{0.1}Ni_{0.9}O_2$ does not influence the discharge capacity;

(ii) the polarization is decreased;

(iii) the discharge capacity is slightly decreased for the sake of an increase in charge voltage.

The major problem in the preparation of $LiNiO_2$ analogs, namely, the strong dependence of Li/Ni ratio on discharge capacity, is solved by the substitution of Ni by Mn.

Acknowledgements

A part of this work was supported by a Grant-in-Aid for Scientific Research (No. 06555138) from the Ministry of Education, Science and Culture, Japan.

References

[1] J.R. Dahn, U. von Sacken, C.A. Michal, Solid State Ionics 44 (1990) 87.
[2] T. Ohzuku, A. Ueda, M. Nagayama, J. Electrochem. Soc. 140 (1993) 1862.
[3] W. Li, J.N. Reimers, J.R. Dahn, Solid State Ionics 67 (1993) 123.
[4] H. Arai, S. Okada, H. Ohtsuka, M. Ichimura, J. Yamaki, Solid State Ionics 80 (1995) 261.
[5] T. Miyashita, H. Noguchi, K. Yamato, M. Yoshio, J. Ceram. Soc. Jpn. 102 (1994) 58.
[6] J.R. Dahn, U. von Sacken, C.A. Michal, J. Solid State Ionics 44 (1990) 87.
[7] R. Kanno, H. Kubo, Y. Kawamoto, T. Kamiyama, F. Izumi, Y. Takeda, M. Takano, J. Solid State Chem. 110 (1994) 216.
[8] I. Davidson, J.E. Greedan, U. von Sacken, C.A. Michal, J.R. Dahn, Solid State Ionics 46 (1991) 243.
[9] Q. Zhong, U. von Sacken, J. Power Sources 54 (1995) 221.
[10] J.N. Reimers, E. Rossen, C.D. Jones, J.R. Dahn, Solid State Ionics 61 (1993) 335.
[11] E. Rossen, C.D.W. Jones, J.R. Dahn, Solid State Ionics 57 (1992) 311.
[12] Y. Nitta, K. Okamura, K. Haraguchi, S. Kobayashi, A. Ohta, J. Power Sources 54 (1995) 511.
[13] M. Yoshio, H. Noguchi, T. Miyashita, H. Nakamura, A. Kozawa, J. Power Sources 54 (1995) 483.
[14] F. Izumi, Nippon Kessho Gakkai Shi 27 (1985) 23.
[15] L.D. Dyer, B.S. Borie Jr., G.P. Smith, J. Am. Chem. Soc. 76 (1954) 1499.
[16] M. Yoshio, H. Noguchi, H. Nakamura, K. Suzuoka, Denki Kagaku 64 (1996) 123.
[17] R.V. Moshtev, P. Zlatilov, V. Manev, A. Sato, J. Power Sources 54 (1995) 329.